

High-Pressure Phase Relations of RbH_2PO_4 , CsH_2PO_4 , and KD_2PO_4

ELIEZER RAPOPORT,* J. B. CLARK, AND P. W. RICHTER

National Physical Research Laboratory, South African Council for Scientific and Industrial Research, P.O. Box 395, Pretoria, South Africa

Received September 22, 1977; in final form November 14, 1977

The phase diagrams of RbH_2PO_4 (RDP), CsH_2PO_4 (CDP), and KD_2PO_4 (DKDP) have been determined to ~40 kbar. Attempts are made to correlate the present phase diagrams with that of KH_2PO_4 and determine which phases are isostructural. The large isotope effect found for KD_2PO_4 is in agreement with the isotope effects in H_2O , D_2O .

Introduction

Potassium dihydrogen phosphate, KH_2PO_4 (KDP), and its alkali phosphate and arsenate isomorphs form an important class of hydrogen-bonded ferroelectrics. This group of substances has been extensively studied (1) especially with respect to their ferroelectric properties. For this reason most of the work has been concentrated at low temperatures around their Curie points.

The high-pressure phase diagrams presenting the phase relations in the high-pressure (40 kbar) high-temperature (~500°C) region have been reported for KH_2PO_4 (2), $\text{NH}_4\text{H}_2\text{PO}_4$ (3), and KH_2AsO_4 (3). The present study is a continuation of the series of alkali dihydrogen phosphates and includes work on RbH_2PO_4 (RDP), CsH_2PO_4 (CDP), and KD_2PO_4 (DKDP). As in the previous studies (2, 3), high pressure was found to suppress dehydration and decomposition processes and to extend the stability range of these substances up to and beyond melting.

RDP belongs to the class of KDP-type compounds where the ferroelectric phase is

orthorhombic space group $C_{2v}^{19}-Fdd2$ and the paraelectric phase is tetragonal space group $D_{2d}^{12}-I42d$ (1). The ferroelectric transition occurs at -126°C , and has been studied at high pressures where the ferroelectric state disappears for $P \geq 15.2$ kbar (4). Numerous (5-11) high-temperature studies have been performed on RDP at atmospheric pressure. These studies confirm a phase transition at $\sim 86^\circ\text{C}$ (6) followed by a dehydration process which occurs at a variety of temperatures between ~ 120 - 200°C . Two authors (7, 10) claim two high-temperature transitions, however, the second transition may be related to the dehydration process. The high-temperature transition at 86°C is quasi-irreversible and the high-temperature phase is reported (6) to be monoclinic and isostructural with the monoclinic phases found for RbD_2PO_4 , KD_2PO_4 , KH_2PO_4 , and CsH_2PO_4 . Far-infrared studies on RDP at room temperature and high pressures yield evidence of a phase transformation at 60 kbar (12). Fritz (13) has reported the pressure dependence of the elastic constants of RDP to 20 kbar at 23°C .

CDP undergoes a recently confirmed ferroelectric transition at -119.5°C (14). The

* Permanent address: Soreq Nuclear Research Centre, Yavne, Israel.

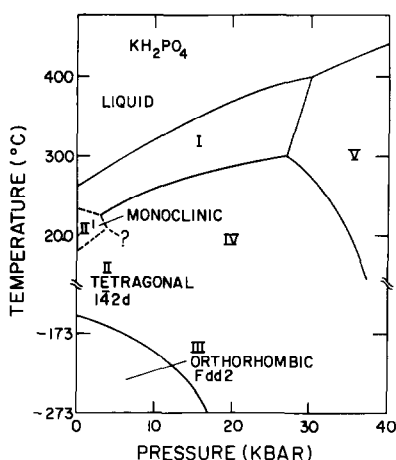


FIG. 1. The phase diagram of KH_2PO_4 from Ref. (30).

main difference, however, is that the paraelectric phase is monoclinic (15) spacegroup $C_{2h}^2-P2_1/m$, and hence does not belong to the KDP-type group where the paraelectric phase is tetragonal (I). Uesu and Kobayashi (15) conclude that the ferroelectricity of CDP takes place through a different atomic structure than that of most KDP-type ferroelectrics.

The phase diagram of KDP has been reported (2), and it is shown in Fig. 1. Recently the influence of partial and complete deuteration on the properties of KDP has occupied much attention. The Curie point changes from 122°K for KDP to 230°K for DKDP (16). These transition temperatures have been studied by a number of workers, and a spread of some 20°K in the values reported for the Curie point of DKDP is certainly due to a lack of complete deuteration (17–19). The pressure dependence of the Curie point has been studied to 24 kbar (20). The effect of deuteration on the high-temperature phase relations has been studied by several authors (7, 8, 11, 21, 22), however, the interpretation of all published results is complicated by two factors. First, at very high deuterium concentrations ($x \gtrsim 0.98$) DKDP can be grown in the monoclinic high-temperature phase at room temperature (21–

23), and second, at higher temperatures DKDP decomposes. The metastable monoclinic phase resists retransformation and apparently does not show the ferroelectric transition to 6°K (22). If the deuterium concentration is lower than ~98% the tetragonal (KDP-type) form appears. This tetragonal form shows the normal ferroelectric behavior as well as the high-temperature transition to the monoclinic form (7, 8, 23) with decomposition following at still higher temperatures (11). As in the case of RDP certain authors (7) report two high-temperature transitions where the higher-temperature transition seems to be linked to a decomposition process. The temperature at which the tetragonal–monoclinic phase transition occurs varies between 65–110°C. Since it is known that for heavily deuterated samples, the monoclinic phase is obtained at room temperature, it would appear that there is some relation between deuteration and the transition temperature. No systematic studies have been conducted in this regard. It is important to note that deuteration of KDP substantially increases the Curie point whereas it seems to substantially lower the tetragonal–monoclinic transition temperature.

Experimental

The RDP used was in the form of single-crystal chips.¹ These single-crystal chips were finely ground prior to use and checked by Guinier X-ray powder diffraction techniques. CDP was prepared by neutralizing solutions of Merck Cs_2CO_3 (purity 99.5%) with H_3PO_4 and methyl orange as an indicator. The solid was precipitated by adding alcohol. The precipitate was filtered, vacuum dried, and baked at 80°C for ~12 hr. The product was excellently crystalline and could be well characterized by Guinier X-ray powder diffraction techniques. DKDP was prepared by dissolving 0.02 mole of Merck (minimum

¹ The RDP was obtained from Dr S. Szapiro of the Soreq Nuclear Research Centre, Yavne, Israel.

TABLE I
PHASE RELATIONS

Phase boundary	Least-squares fit (P in kbar)	Standard deviation ($^{\circ}\text{K}$)
RbH_2PO_4 II/I	$t (^{\circ}\text{C}) = 281 + 5.125 P - 0.05715 P^2$	1.7
RbH_2PO_4 V/I	$t (^{\circ}\text{C}) = 350 + 7.143 (P - 16.4) - 0.0919 (P - 16.4)^2$	1.9
RbH_2PO_4 V/Liquid	$t (^{\circ}\text{C}) = 402 + 3.909 (P - 24.4) - 0.0270 (P - 24.4)^2$	2.0
RbH_2PO_4 I/Liquid	$t (^{\circ}\text{C}) = 292.1 + 9.175 P - 0.1955 P^2$	1.9
CsH_2PO_4 II/I	$t (^{\circ}\text{C}) = 230 + 2.80 P$	3.0
CsH_2PO_4 V/I	$t (^{\circ}\text{C}) = 262 + 8.716 (P - 11) - 0.1107 (P - 11)^2$	2.9
CsH_2PO_4 V/VI	$t (^{\circ}\text{C}) = 384.9 + 2.016 (P - 29.9)$	2.5
CsH_2PO_4 VI/I	$t (^{\circ}\text{C}) = 384.9 + 6.998 (P - 29.9) - 0.0828 (P - 29.9)^2$	2.0
CsH_2PO_4 VI/Liquid	$t (^{\circ}\text{C}) = 457 - 0.0411 (P - 42)$	0.7
CsH_2PO_4 I/Liquid	$t (^{\circ}\text{C}) = 345.7 + 8.340 P - 0.1405 P^2$	4.1
KD_2PO_4 I/Liquid	$t (^{\circ}\text{C}) = 250 + 7.334 P - 0.1081 P^2$	1.9
KD_2PO_4 V/Liquid	$t (^{\circ}\text{C}) = 368.5 + 4.883 (P - 25) - 0.0724 (P - 25)^2$	1.4

purity 99%) grade KH_2PO_4 in 2 ml D_2O obtained from Norsk Hydro-elektrisk (purity 99.7%). The solution was vacuum dried and the process repeated with 8 and 7 ml of D_2O . The resulting material thought to be practically 100% deuterated was stored in a vacuum desiccator over silica gel and was used for the high-pressure experiments within 48 hr.

Pressures of up to 45 kbar were generated in a piston-cylinder apparatus (24). The supported piston design (25) was used above 40 kbar. Phase transformations were studied by means of differential thermal analysis (DTA) with Chromel-Alumel thermocouples and volumetric techniques. The detailed experimental techniques have been described previously (28–30). The samples were contained in Ni and Cu capsules. X-ray diffraction confirmed that no contamination had taken place in either of the capsule materials. The majority of experiments were done in the capsules that yielded the most favorable signals, these being Ni for CDP and Cu for RDP and DKDP. In all of the experiments where the melting curve was studied, thermal overshoot was minimized to prevent sample decomposition. In certain cases the melting temperature was exceeded by $\sim 50^{\circ}\text{C}$ to scan the higher-temperature zone, and even these

runs showed no evidence of decomposition. Heating/cooling rates used varied between 0.2 – $1.5^{\circ}\text{C}/\text{sec}$.

In general the phase boundaries are believed to be known to ± 0.5 kbar and $\pm 2^{\circ}\text{C}$ unless otherwise stated. The least-squares fits of all phase boundaries and the coordinates of the triple points are given in Tables I and II.

Experimental Results

RbH_2PO_4

The complete phase diagram of RDP is shown in Fig. 2. Studies were made at atmospheric pressure with a differential scan-

TABLE II
COORDINATES OF TRIPLE POINTS

Triple point	P (kbar)	T ($^{\circ}\text{C}$)
RbH_2PO_4 II/V/I	16.4	350
RbH_2PO_4 I/V/Liquid	24.4	402
RbH_2PO_4 II/III/V	Cannot be determined from present data	
CsH_2PO_4 I/II/V	11.0	262
CsH_2PO_4 II/III/V	11.2	148
CsH_2PO_4 I/V/VI	29.9	384.9
CsH_2PO_4 I/VI/Liquid	42.0	457
KD_2PO_4 I/V/Liquid	25.0	368.5

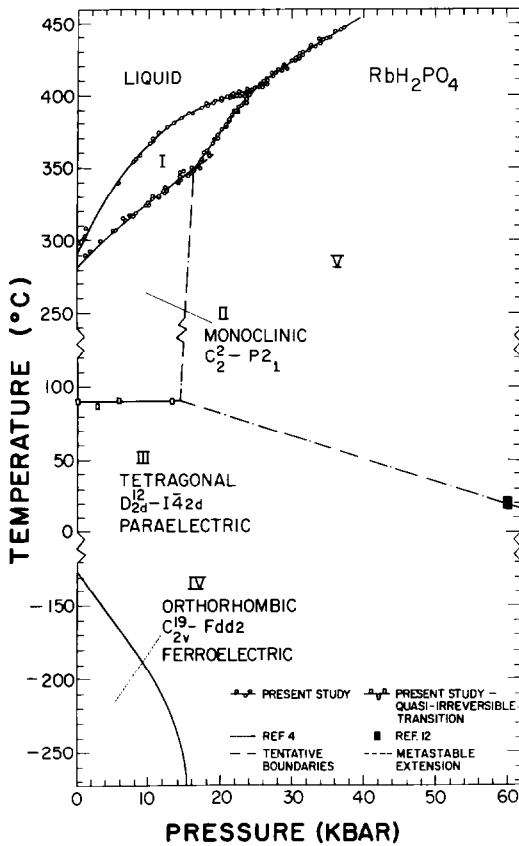


FIG. 2. The phase diagram of RbH_2PO_4 to 60 kbar.

ning calorimeter (DSC) (29). Although the results are not clear-cut they strongly suggest a single quasi-irreversible transition over a range in temperature (86–111°C) with an enthalpy of 4.665 kJ/mole. The sample shows clear evidence of decomposition after the transition has occurred and this factor complicates matters considerably. Additional complications such as temperature nonuniformity due to sample size are discussed (29).

The quasi-irreversible transition was clearly seen as a single transition at high pressures at 90°C. Its quasi-irreversible nature was confirmed and in each high-pressure experiment only one signal was obtained on this boundary. Typical signals are shown in Fig. 3(i) and (ii). A comparison of these signals shows that at ~13 kbar the signal is considerably smaller. The points plotted on the III/II

boundary in Fig. 2 could be reproduced from run to run. On raising the temperature beyond the III/II transition, large signals were found (Fig. 3(iii)) corresponding to a new II/I solid-solid transition taking place at 281°C at atmospheric pressure. A hysteresis of some 10–18°C was encountered and only heating signals are plotted in Fig. 2. The II/I phase boundary rises with an initial slope of 5.1°C/kbar and very little curvature to 16.4 kbar, 350°C, where a sharp change in slope and signal size and shape (Fig. 3(iv)) indicated the presence of a new RbH_2PO_4 II/V/I triple point. The resulting V/I phase boundary rises steeply and thermal overshoot yields a second set of signals at higher temperatures corresponding to the melting of RbH_2PO_4 I (Fig. 3(v)) ($T_m = 292^\circ\text{C}$ at atmospheric pressure). Increasing pressure forces the two boundaries to meet at the RbH_2PO_4 I/V/Liquid triple point at 24.4 kbar, 402°C. From this triple point the melting curve of RbH_2PO_4 V rises at ~3.9°C/kbar to the maximum pressure reached of 38 kbar. The cooling signals obtained on the V/Liquid boundary showed an interesting feature illustrated in Fig. 3(vi). If the melting temperature was exceeded by ~20°C close to the I/V/Liquid triple point a double cooling signal was obtained, the lower one showing substantial supercooling behavior. If, however, the melting process was not completed this double signal was not obtained. The behavior was checked a number of times and is possibly due to metastability associated with the I/V/Liquid triple point. Data obtained on the II/I and I/Liquid boundaries below 4 kbar were obtained on releasing and increasing pressure and there was no evidence of any decomposition which was confirmed by *post mortem* X-ray analysis. Figure 2 also includes data on the ferroelectric IV/III transition from Percy and Samara (4), and the high-pressure infrared data from Blinc *et al.* (12) which confirm the presence of a high pressure transition at ~60 kbar.

Volumetric data were collected at 20 and 58°C but there was no evidence of any high-

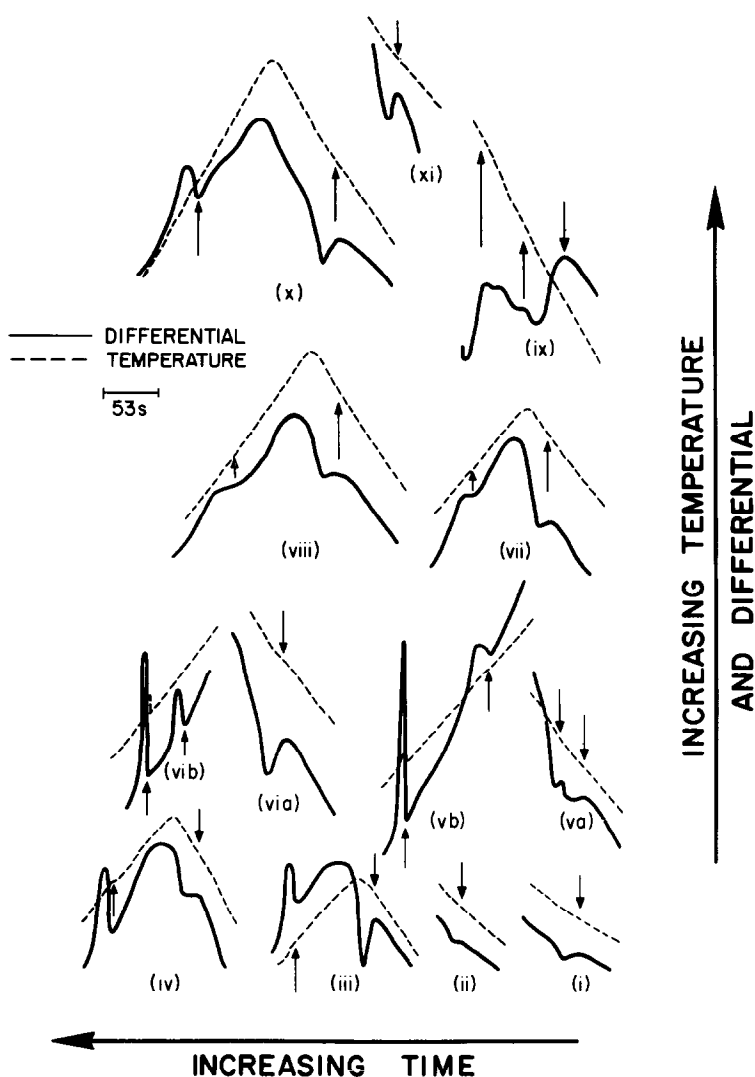


FIG. 3. Typical DTA signals obtained for RbH_2PO_4 . (i) RDP III/II 2.8 kbar 87°C. (ii) RDP III/II 13.2 kbar 90.4°C. (iii) RDP II/I 3.2 kbar 299°C cooling signal depressed. (iv) RDP V/I 18.9 kbar 366°C cooling signal depressed. (v) (a) RDP V/I + I/Liq at 22.3 kbar 389 and 401°C heating. (b) RDP I/Liq + V/I at 22.3 kbar 397 and 349°C note substantial super cooling and direct thermal arrest. (vi) (a) RDP V/Liq 26.9 kbar 407°C heating + overshoot. (b) RDP V/Liq 26.9 kbar 399.7 and 372.4°C showing unusual double cooling signal behavior when melting point overshoot. (vii) CDP II/I at 2.0 kbar, 234°C. (viii) CDP V/I at 18.5 kbar, 321°C, (ix) CDP at 39 kbar showing V/VI transition at 403°C, VI/I at 443°C and I/Liq at 461°C. (x) CDP I/Liq at 10.3 kbar, 421°C. (xi) DKDPI/Liq at 16 kbar, 338.5°C.

volume change transitions to 38 kbar. The position of the II/III/V triple point and the slopes of the II/V and III/V boundaries could not be determined from the present data. The volumetric data at 58°C can only be said to provide a limiting condition. The complete

phase relations and triple point coordinates are listed in Tables I and II.

CsH_2PO_4

The complete phase diagram of CDP is shown in Fig. 4. Atmospheric pressure DSC

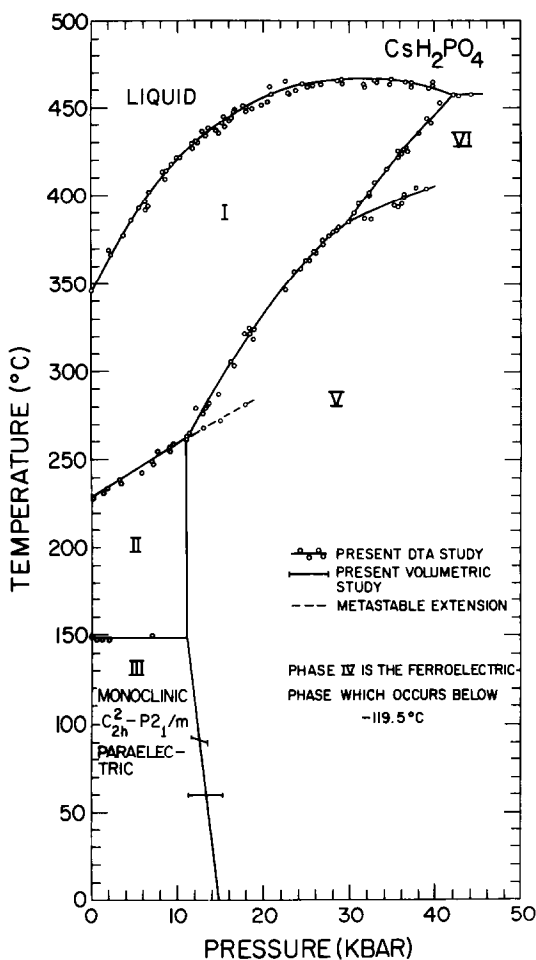


FIG. 4. The phase diagram of CsH_2PO_4 to 45 kbar.

studies revealed two transitions (29). A quasi-irreversible transition was found at 149°C with an enthalpy of 1.071 kJ/mole and a second reversible transition was found at 230°C with an enthalpy of 7.615 kJ/mole. Decomposition occurred soon after the second transition.

Very faint signals were obtained at high pressures on the III/II boundary. The quasi-irreversible nature of the transition was confirmed. In the higher-temperature region pressure was raised to at least 5 kbar before raising the temperature to prevent decomposition. Points below 5 kbar were obtained on releasing pressure and *post mortem* X-ray analyses confirmed that there was no evidence

of sample decomposition in any of the high-pressure experiments. The CDP II/I transition (Fig. 3(vii) shows typical signals) rises with an initial slope of $3.6^\circ\text{C}/\text{kbar}$ to 11 kbar, 262°C , where there is a sharp change in slope indicating a triple point. The exact position of the triple point is difficult to determine on increasing pressure, as the II/I transition can be followed metastably for ~ 8 kbar beyond the triple point. However, on decreasing pressure the new V/I boundary shows clearly where the break occurs. The V/I transition yields slightly broader signals (Fig. 3(viii)) than the II/I transition, and the cooling signals were $\sim 20^\circ\text{C}$ lower than heating signals versus $\sim 25\text{--}30^\circ\text{C}$ for the II/I transition. Only heating signals are plotted in Fig. 4. The V/I phase boundary rises with an initial slope of $8.7^\circ\text{C}/\text{kbar}$ from the I/II/V triple point to ~ 29.9 kbar, where another sharp slope change and a new set of signals are evidence of another triple point. The I/V/VI triple point is located at 29.9 kbar, 384.9°C . If pressure is raised still further and temperature is allowed to overshoot the VI/I transition, a set of signals can be found which have been attributed to the melting of CDP I. The VI/I and I/Liquid boundaries meet at a I/VI/Liquid triple point at 42 kbar, 457°C . The V/VI transition rises at a lower rate but evidence suggests that the melting curve of CDP VI is fairly flat, and therefore the V/VI boundary can be expected to meet the VI/Liquid boundary at the V/VI/Liquid triple point which we estimate in the region of 65 kbar, 457°C . Figure 3(ix) shows examples of typical signals where the V/VI, VI/I, and I/Liquid transitions can be seen.

The melting curve of CDP is most interesting. It rises with an initial slope of $8.3^\circ\text{C}/\text{kbar}$ and then passes through a broad maximum. The exact position of the maximum is difficult to estimate. From the least-squares fit of the complete data set it is estimated at 29.7 kbar, 469°C . However, on inspection of the data a value of 32 kbar, 467°C seems more acceptable. Several runs were made to ensure that the

melting curve did pass through a maximum and that no triple point existed in the 20-kbar region. The temperature was raised to $\sim 550^\circ\text{C}$ at a number of pressures in the region of 20 kbar, but no evidence of any further boundaries was found. It is important to note that even at 550°C at 20 kbar no decomposition was found, showing how well pressure has stabilized the compound. Figure 3(x) shows a good melting signal obtained, but some signals tended to be broader. Supercooling was not found to be present although cooling signals were $\sim 10^\circ\text{C}$ lower.

In addition to the DTA studies, volumetric studies were carried out to confirm the II/V/I triple point and the resulting III/V and II/V phase boundaries. The results show that a phase transition does occur, but that it is very sluggish at room temperature as was found to be the case previously for $\text{NH}_4\text{H}_2\text{PO}_4$ (3). Volumetric studies at room temperature showed no sign of any transition, however, work at 60 and 90°C yielded conclusive evidence of the transition. In view of reservations concerning piston rotation (28) the data are summarized in Table III. The volumetric data yield a volume change of 1.6% or $1.12\text{ cm}^3/\text{mole}$. Figure 4 shows that the present volumetric data ties in well with the break in the II/I phase boundary and two triple points (I/II/V and II/III/V) are shown. The volumetric studies were not attempted at $T > 100^\circ\text{C}$ so no data was obtained on the

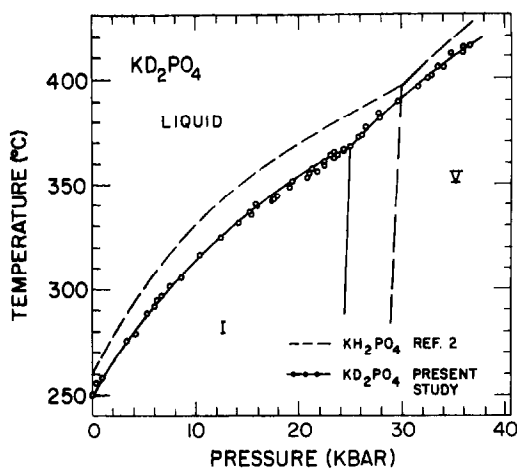


FIG. 5. The melting curve of KD_2PO_4 .

II/V boundary. The complete phase relations are summarized in Tables I and II.

KD_2PO_4

The results obtained for DKDP showed two major differences when compared with KDP. The solid-solid transitions found for KDP (2) did not appear. The melting point for DKDP, with only a clamping pressure applied was found to be 250°C compared with 260°C for KDP. The results obtained on the melting curve are shown in Fig. 5, which also shows the melting curve of KH_2PO_4 from Ref. (2). A substantial variable depression of the melting point was found which varied between 10°C at atmospheric pressure and 18°C at ~ 16 kbar. The KH_2PO_4 I/V/Liquid triple point is

TABLE III
PISTON DISPLACEMENT DATA^a FOR CsH_2PO_4

Temperature	Start of transition increasing pressure (kbar)	After 4 cycles piston rotation at the transition (kbar)	Start of transition decreasing pressure (kbar)	After 4 cycles piston rotation at the transition (kbar)	Friction as determined from piston rotation away from transition (kbar)
Upstroke 60°C Downstroke	16.0	13.2	10.6	11.2	0.7
Upstroke 90°C Downstroke 93°C	14.3	12.7	10.8	11.4	0.8

^a For reasons concerning the presentation of data in present form see Ref. (28).

situated at 30.1 kbar, 397°C, whereas the equivalent triple point for KD_2PO_4 is found at 25 kbar, 368°C. A typical signal obtained is shown in Fig. 3(xi). Cooling signals were $\sim 30^\circ\text{C}$ below melting and only melting signals are plotted in Fig. 5. The complete phase relations are summarized in Tables I and II.

Discussion

A clear understanding of the high-pressure crystal chemistry of the KDP-type compounds is hampered by a lack of high-temperature structural data at atmospheric pressure. KDP itself seems to dictate a pattern of phase behavior where the ferroelectric orthorhombic phase III transforms to the paraelectric tetragonal phase II which transforms to a monoclinic high temperature phase II'. The unusual decrease in symmetry on the II/II' transition with increasing temperature is worth noting. The final high-temperature phase I prior to melting has not been satisfactorily characterized. The present work on RDP confirms the trend and it can only be assumed that the high-temperature phases RDP I and KDP I are isostructural. This is strongly supported by the initial slopes of the melting curves in each case, being 9.2 and 9.6°C/kbar for RDP and KDP, respectively.

No entropy values for melting are available because of decomposition prior to melting at atmospheric pressure so all thermodynamic calculations done refer to the solid–solid transitions. The RDP III/II transition at 90°C has an enthalpy of 4.665 kJ/mole (29). This refers to an entropy change of 12.85 J/mole $^\circ\text{K}$. The observed slope is practically 0°C/kbar which implies a zero or very small volume change on the phase boundary. No data are available on the lattice parameters of the monoclinic phase of RDP but some estimates may be obtained from recent data on KDP and DKDP (22, 23). Using the reported lattice parameters a volume change of ~ 0.6 cm 3 /mole can be calculated for the isostructural KDP transition which confirms the very

small volume change associated with the transition.

CDP is slightly more promising. On the quasi-irreversible III/II transition at 149°C an enthalpy of 1.071 kJ/mole is found (29) which refers to an entropy change of 2.54 J/mole $^\circ\text{K}$. The high-pressure behavior of the CDP III/II transition yields a slope of $\sim 0^\circ\text{C}/\text{kbar}$ which implies a zero or very small volume change from the Clausius–Clapeyron equation. At higher temperatures the CDP II/I phase transition has an associated entropy change of 15.13 J/mole $^\circ\text{K}$. This boundary has an initial slope of 2.80°C/kbar which implies a volume change of 0.4 cm 3 /mole. Assuming that the entropy change remains approximately constant on the II/I boundary, we can use the observed slope of the II/I boundary (\sim straight line) at the triple point to calculate the volume change at the triple point as 0.4 cm 3 /mole. On the II/V and III/V boundaries the exact location of the II/III/V triple point cannot be precisely determined, however, the measured volume change on the III/V boundary is not expected to change much as it carries over on to the II/V boundary. We can therefore assume that the determined $\Delta V_{\text{III/V}}$ is approximately the value for $\Delta V_{\text{II/V}}$ at the I/II/V triple point. Using the additive relations at the I/II/V triple point, $\Delta V_{\text{V/I}}$ is found to be 1.54 cm 3 /mole. Combining this with the observed slope on the V/I boundary an entropy of 17.7 J/mole $^\circ\text{K}$ can be determined from the Clausius–Clapeyron equation. Unfortunately no enthalpy data are available on the melting curve, so the present calculations cannot be extended to include the triple points at higher pressure.

In obtaining an overview of the crystal chemistry, the empirical rule (30), that increased cationic size simulates increased pressure, is of substantial value in the present case. The sequence along the pressure axis would be K, Rb, and then Cs. The problem that arises immediately is how to fit in the KDP II' phase (notation from Ref. (2)) with the present RDP II. From Rapoport (2), the

complexity of the phase relations between 150–250°C below 8 kbar is quite apparent. The most important complicating feature is the quasi-irreversible tetragonal–monoclinic transition. If we compare the phase diagrams of KDP and RDP we find that the only region which is dissimilar is the KDP diagram below ~5 kbar. However, RDP is expected to be similar to the higher-pressure portion of the KDP phase diagram. This immediately raises the possibility that KDP IV could be isostructural with RDP II. The tentative (2) KDP II/IV phase boundary was not found in high-pressure acoustic measurements (13), confirming the original P.V.T work (2) and compressibility measurements (31). If this boundary had a flatter slope which is thermodynamically possible it would explain why it has not been observed and it could then be the counterpart of the RDP II/III boundary. The average slopes of the KDP IV/I and RDP II/I boundaries are 3.4 and 4.2°C/kbar, respectively, which are similar. The incomplete crystallographic data and considerations of kinetics and the quasi-irreversible nature of the KDP II/II' and RDP III/II transitions tend to suggest that KDP II' is isostructural with RDP II. High-pressure high-temperature X-ray studies are needed to differentiate between the two possibilities. The isostructural phases are listed in Table IV.

The RDP II/III/V triple point could also be expected to have a counterpart and would involve the KDP IV, II, and V phases. Such a triple point would then automatically raise the

pressure at which KDP II/V transition can be expected at room temperature. This would agree well with the work of Fritz (13) and Blinc *et al.* (12). The present discussion confirms the need for additional high-pressure work on KDP in the region 150–250°C below 10 kbar to establish the exact phase relations. Any additional work will however be hampered by the nature of the quasi-irreversible tetragonal–monoclinic phase transition.

The phase relations of CDP are substantially different as regards the paraelectric monoclinic phase. However, certain portions of the phase diagram could be related to those obtained for KDP and RDP. The initial slope of the melting curve is 8.3°C/kbar which could easily link it to the higher-pressure portions of the KDP and RDP melting curves. This could imply that CDP I is isostructural with KDP I and RDP I and that the CDP II/I boundary is the counterpart of the RDP II/I and the KDP IV/I boundaries. The initial slope of the CDP II/I boundary is 3.6°C/kbar and thus agrees well. The CDP III/II transition has exactly the same character (quasi-irreversible) as the KDP II/II' and RDP III/II and it is very tempting to assume some relationship. However, the fact that CDP II is monoclinic whereas KDP II and RDP III are tetragonal complicates matters considerably. It is possible that the monoclinic CDP phase is related to the tetragonal KDP and RDP phases. However, the exact relationship is not clear. Additional structural data are required on CDP to clarify matters. The phase diagram of CDP at high pressures and temperatures shows many new features including the maximum in the melting curve plus the CDP V/VI boundary.

The remarkably strong effect of deuteration on the phase relations of KDP is most interesting. At low temperatures the Curie point for KDP is 122 and 230°K for DKDP. The transition mechanism and the large deuteration effects have been accounted for by the coupled-mode model (32). The effect of deuteration extends to other aspects as well,

TABLE IV

PROPOSED ISOSTRUCTURAL PHASES FOR RDP AND KDP

RDP	KDP	Structure
IV	III	Ferroelectric Orthorhombic C_{2v}^2-Fdd2
III	II	Paraelectric Tetragonal $D_{2d}^{12}-I\bar{A}2d$
II	II' or IV	Monoclinic $C_2^2-P2_1$
I	I	Unknown

namely, that the monoclinic high-temperature phase exhibits a major extension of its stability zone plus the fact that recent work (22) shows that monoclinic DKDP does not undergo the ferroelectric phase transition to 6°K. The monoclinic-tetragonal phase transition has been linked to changes in the hydrogen bond (7) and hence such dramatic effects are tentatively expected. Previous work (33, 34) on deuteration effects on melting and solid-solid transitions include studies on the H₂O and D₂O phase diagrams. The largest isotope effect (33, 34) showed the ice VI/VII and VI/VIII boundaries ~1.3 kbar apart (D₂O lower). The melting curve of D₂O although seeming to be higher in temperature is slightly depressed when the 1.3-kbar pressure effect is taken into account. The present work shows the melting curve of DKDP lower than that of KDP, with a pressure shift of ~5 kbar at 30 kbar.

Acknowledgments

The authors would like to thank Mr. A. Kingon, Mrs. I. Strijdom, and Mrs. L. du Toit for technical assistance, J. J. Erasmus and A. de Kleyn and their personnel for the upkeep of the apparatus and the manufacture of the furnace assemblies. Calculations were done on the CDC 174 computer of the National Research Institute of Mathematical Sciences using programs written by Mrs. M. C. Pistorius. The authors would also like to thank Dr. S. Szapiro of the Soreq Nuclear Research Centre, Israel, for single-crystal chips and Dr. P. K. Gallagher of Bell Laboratories for additional thermal analysis data.

References

1. An excellent collection of data on these compounds is contained in Vols. III/3 and III/9 of the Landolt-Börnstein New Series on Crystal and Solid State Physics: T. MITSUI *et al.* "Ferro and Antiferroelectric Substances" (K.-H. Hellwege and A. M. Hellwege, Eds.), Springer-Verlag, Berlin, 1969, 1975.
2. E. RAPOPORT, *J. Chem. Phys.* **53**, 311 (1970).
3. J. B. CLARK, *High Temp. High Pressures* **1**, 553 (1969).
4. P. S. PEERCY AND G. A. SAMARA, *Phys. Rev. B* **8**, 2033 (1973).
5. L. ERDEY, G. LIPTAY, AND S. GÁL, *Talanta* **12**, 883 (1965).
6. R. BLINC, D. E. O'REILLY, E. M. PETERSON, AND J. M. WILLIAMS, *J. Chem. Phys.* **50**, 5408 (1969).
7. J. GRÜNBERG, S. LEVIN, I. PELAH, AND D. GERLICH, *Phys. Status Solidi B* **49**, 857 (1972).
8. L. P. PEREVERZEVA, N. Z. POGOSSKAYA, YU. M. POPLAVKO, V. I. PAKHOMOV, I. S., REZ, AND G. B. SIL'NITSKAYA, *Fiz. Tverd. Tela* **13**, 3199 (1971).
9. B. OREL AND D. HADŽI, *J. Mol. Struct.* **18**, 495 (1973).
10. V. A. D'YAKOV, V. A. KOPTSIK, I. V. LEBEDEVA, A. V. MISCHENKO, AND L. N. RASHKOVICH, *Kristallografiya* **18**, 1227 (1973).
11. P. K. GALLAGHER, *Thermochim. Acta* **14**, 131 (1976).
12. R. BLINC, J. R. FERRARO, AND C. POSTMUS, *J. Chem. Phys.* **51**, 732 (1969).
13. I. J. FRITZ, *Phys. Rev. B* **13**, 705 (1976).
14. A. LEVSTIK, R. BLINC, P. KADABA, S. ČIZIKOV, I. LEVSTIK, AND C. FILIPIČ, *Ferroelectrics* **14**, 703 (1976).
15. Y. UESU AND J. KOBAYASHI, *Phys. Status Solidi A* **34**, 475 (1976).
16. G. M. LOIACONO, J. F. BALASCIO, AND W. OSBORNE, *Appl. Phys. Lett.* **24**, 455 (1974).
17. H. UMEBAYASHI, B. C. FRAZER, G. SHIRANE, AND W. B. DANIELS, *Solid State Commun.* **5**, 591 (1967).
18. A. BADDUR, B. A. STRUKOV, I. A. VELICHKO, AND V. N. SETKINA, *Kristallografiya* **17**, 1065 (1972).
19. E. N. VOLKOVA, Y. S. PODSHIVALOV, L. N. RASHKOVICH, AND B. A. STRUKOV, *Izv. Akad. Nauk SSSR Ser. Fiz.* **39**, 787 (1975).
20. G. A. SAMARA, *Ferroelectrics* **7**, 221 (1974).
21. J. Y. NICHOLSON AND J. F. SOEST, *J. Chem. Phys.* **60**, 715 (1974).
22. N. S. J. KENNEDY, R. J. NELMES, F. R. THORNLEY, AND K. D. ROUSE, *Ferroelectrics* **14**, 591 (1976).
23. A. TOMAS, P. HERPIN, AND J. DOUCET, *Bull. Soc. Fr. Minéral. Cristallogr.* **98**, 341 (1975).
24. G. C. KENNEDY AND P. N. LAMORI, in "Progress in Very High Pressure Research" (F. P. Bundy, W. R. Hibbard, and H. M. Strong, Eds.), pp. 304-313, Wiley, New York (1961).
25. J. HAYGARTH AND G. C. KENNEDY, *Rev. Sci. Instrum.* **38**, 1590 (1967).
26. P. W. RICHTER AND C. W. F. T. PISTORIUS, *J. Solid State Chem.* **3**, 197 (1971).
27. C. W. F. T. PISTORIUS AND J. B. CLARK, *High Temp. High Pressures* **1**, 561 (1969).
28. A. B. WOLBARST, J. B. CLARK, AND P. W. RICHTER, *Rev. Sci. Instrum.*, in press.
29. B. METCALFE AND J. B. CLARK, *Thermochim. Acta*, submitted for publication.

30. C. W. F. T. PISTORIUS, in "Progress in Solid State Chemistry" (J. McCaldin and G. Somorjai, Eds.), Vol. 11, part 1, Pergamon, New York (1976).
31. P. MOROSIN AND G. A. SAMARA, *Ferroelectrics* **3**, 49 (1971).
32. P. S. PEERCY, *Phys. Rev. B* **13**, 3945 (1976).
33. J. P. JOHARI, A. LAVERGNE, AND E. WHALLEY, *J. Chem. Phys.* **61**, 4292 (1974).
34. C. W. F. T. PISTORIUS, E. RAPOPORT, AND J. B. CLARK, *J. Chem. Phys.* **48**, 5509 (1968).